International Journal of Science and Engineering Applications
Volume 13-Issue 06, 01 - 03, 2024, ISSN:- 2319 - 7560
DOI:10.7753/IJSEA1306.1001

Study on Mechanism and Kinetics of the H_2O-Abstraction Reactions Between C_3H_4 Isomers and $^{\bullet}OH$ Radicals

Tien V. Pham
School of Chemistry and Life Sciences
Hanoi University of Science and Technology
Hanoi City, Vietnam

Abstract: Isomers of C_3H_4 play an important role in various chemical environments. In combustion processes, the reactions of hydroxyl radicals with C_3H_4 isomers are critical in the overall fuel oxidation system. In the present work, mechanism and rate constants of $^{\bullet}OH$ radicals with allene ($H_2C{=}C{=}CH_2 + {}^{\bullet}OH \rightarrow H_2C{=}C{=}CH^{\bullet} + H_2O$) and propyne ($CH_3C{\equiv}CH + {}^{\bullet}OH \rightarrow {}^{\bullet}CH_2C{\equiv}CH + H_2O$) were calculated using the DFT/B3LYP and TST approaches. Results show that propyne reacts faster with $^{\bullet}OH$ radical than allene at low and moderate temperatures ($T \leq 1000$ K), opposite to the results at higher temperature regions.

Keywords: Allene; Propyne; DFT; hydroxyl radicals; TST

1. INTRODUCTION

Numerous mechanisms governing the thermal conversion of isomers on the C_3H_4 surface are pivotal in organic chemistry. Consequently, they serve not only as templates for larger systems but also establish a fundamental framework for hydrocarbon reactions.

The interactions between allene ($H_2C{=}C{=}CH_2$) and propyne ($CH_3C{\equiv}CH$) with hydroxyl radicals ($^{\bullet}OH$) are significant across a spectrum of chemical environments, ranging from combustion to atmospheric and astrophysical realms.[1-2] At moderate to high temperatures, allene and propyne emerge as key intermediate species in combustion systems, where their reactions profoundly influence the formation of polyaromatic compounds, potential precursors to soot particles.[3-5] Notably, these reactions may yield propargyl radical ($^{\bullet}C_3H_3$), the smallest resonantly stabilized hydrocarbon radical, initiating the formation of the initial aromatic ring.[6-10] Consequently, the interactions of hydroxyl radicals with allene and propyne play a pivotal role in the comprehensive oxidation pathway of these molecules.[11]

Many experiments and calculations have been undertaken to elucidate the chemical kinetics of allene and propyne.[12-15] Nevertheless, investigations into the reactions of these two species with $^{\bullet}OH$ radicals are still limited. Several previous experimental works have investigated gas-phase reactions of $^{\bullet}OH$ radicals with allene and propyne at ambient temperature and relatively low pressures. At 298 ± 3 K, rate constants of the reactions allene + $^{\bullet}OH$ (1) and propyne + $^{\bullet}OH$ (2) were found to rise from ~2.5 to 9.8×10^{-12} and from 0.95 to 6.21×10^{-12} cm^3 $molecule^{-1}$ s^{-1}, respectively.[16-18]

Zádor and Miller[15] recently conducted an extensive ab initio theoretical investigation, delineating the potential energy surface of C_3H_5O for the reactions (1) and (2). They computed rate constants for direct hydrogen abstraction and $^{\bullet}OH$ radicals addition to the double or triple bonds. Their findings indicated that at elevated temperatures (>1000 K), the key path for the bimolecular reactions (1) and (2) is the formation of propargyl radical with water molecule. However, at lower temperatures, the chemistry becomes more intricate, involving a competition between adduct stabilization, isomerization, and dissociation processes.

In the current work, the H_2O-abstraction reactions of $^{\bullet}OH$ radicals with allene and propyne have been conducted at a wide range of temperatures (300 - 2000 K). Optimizations were carried out using DFT/B3LYP, while calculations for rate constants were performed by TST approach.

2. COMPUTATIONAL METHODS

In this study, we used the DFT/B3LYP functional along with the Pople basis set 6-311++G(3df,2p) to optimize geometric structures of all species of the C_3H_4 + $^{\bullet}OH$ reactions. Vibrational frequencies and zero-point vibrational energies (ZPVE) corrections are obtained at the same level of theory. The stationary points are identified for local minima or transition states according to their vibrational analysis, in which, the reactants, intermediates, and products possess all real frequencies, whereas a transition state has only one imaginary frequency. Transition states were verified by intrinsic reaction coordinate (IRC) calculations for the connectivity of the reactants and products. The energies of these species were then refined by using the CCSD(T) method in conjunction with the Dunning basis sets aug-cc-pV(T + D)Z. All the calculations were conducted by the software package Gaussian 16.

Rate constants of the system have been predicted based on the model of transition state theory (TST). The quantum mechanics tunneling effect has also been considered in this case. Therefore, the formula used to calculate rate constants has the form as follows:

$$k_r = \chi \frac{k_B T}{h} \frac{q^*}{q_1 q_2} e^{-E_0^*/RT}$$

where χ is transmission coefficient; q^*, q_1, q_2 are sum of state of transition state, reactant A, and reactant B, respectively; E^* is activation energy; R and T are ideal gas constant and Kelvin temperature, respectively; k_B and h are Boltzmann and Planck constant, respectively.

3. RESULTS AND DISCUSSION

In this study, we only care about the formation of propargyl radicals and water molecule when conducting the reactions between C_3H_4 and $^{\bullet}OH$ radicals. Therefore, two following reactions have been considered carefully.

International Journal of Science and Engineering Applications
Volume 13-Issue 06, 01 - 03, 2024, ISSN:- 2319 - 7560
DOI:10.7753/IJSEA1306.1001

$CH_2 = C = CH_2 + {}^{\bullet}OH \rightarrow CH_2 = C = CH^{\bullet} + H_2O$ (1)

$CH_3 - C \equiv CH + {}^{\bullet}OH \rightarrow {}^{\bullet}CH_2 - C \equiv CH + H_2O$ (2)

Based on these two reactions, geometric structures of all species involved have been built by using Gaussview 6. And then they were optimized at the B3LYP/6-311++G(3df,2p) level with the use of Gaussian 16. The energies of them were refined at the CCSD(T)/aug-cc-pV(T+D)Z level of theory with ZPE corrections. These values are shown in Figure 1.

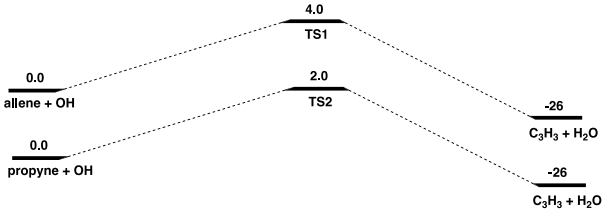

Figure 1. Abstraction paths of the reactions between C_3H_4 isomers and ${}^{\bullet}OH$ radicals.

As shown in Figure 1, both the reaction channels proceed via one transition state, in which the first one (allene + ${}^{\bullet}OH$) goes through the TS1 transition state with barrier height of 4.0 kcal/mol, while the second one (propyne + ${}^{\bullet}OH$) occurs via the TS2 transition state with barrier height of 2.0 kcal/mol. Thus, it can be said that the H_2O-abstraction process of the latter is dominant compared to that of the former and these two channels can take place quickly under embient conditions because the energy barriers of them are very small. This result seems reasonable because separating H atom from the CH_3 group of propyne is easier than that from the CH_2 group of allene. Geometric structures of the two transition states TS1 and TS2 shown in Figure 2 indicate that ${}^{\bullet}OH$ radicals attack hydrogen atoms of the two groups CH_2 and CH_3 at different distances. The first one is about 1.5 Å which is just over 0.1 Å less than the second one, whereas the C … H distances of TS1 and TS2 are not significantly different (1.15 versus 1.13 Å).

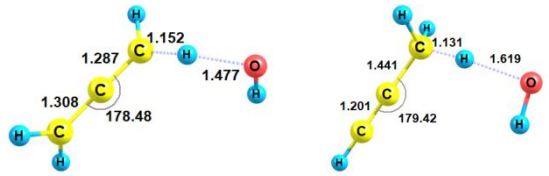

TS1 TS2

Figure 2. Geometric structures of the transition states of the reactions between C_3H_4 isomers and ${}^{\bullet}OH$ radicals.

Imaginary frequencies recorded at the time of ${}^{\bullet}OH$ attack on allene and propyne are 316 and 108 cm^{-1}, respectively, which show that the first TS vibrates stronger than the second TS. In other words, the TS1 saddle point consumes more energy to break the C - H bond compared to the TS2 saddle point. In addition, to facilitate the OH attack on C_3H_4 isomers, the bond angle ∠CCC of both TSs have reduced slightly about 1 or 2º, while the bonds of C-C and C-H are nearly unchanged in comparison with those in the structures of allene and propyne.

It is worth noting that the products of the two reactions are the same, both containing propargyl radical and water molecule ($C_3H_3 + H_2O$) with energy of 26 kcal/mol under the reactants. The propargyl radicals, once formed, may undergo self-reaction to yield benzene aromatic ring molecules which are crucial compounds in the synthesis of polycyclic aromatic hydrocarbons (PAHs).

To assess the validity of our single referenced outcomes, we conducted a T1 diagnostic analysis to gauge the extent of multireference character within the wave function. The findings pertaining to the reactants, products, and transition states involved in the reactions (1) and (2) are outlined in Table 1. The calculated results indicate that the T1 diagnostics for all species exhibit negligible multireference character, as evidenced by values of singlet and doublet states below 0.015 and 0.035, respectively (the threshold for T1 diagnostic of a closed-shell species being 0.02, while that for open-shell species is approximately 0.045). This suggests that single-reference methods can be reliably applied in our current investigation. Additionally, examination of Table 1 reveals that spin contamination values for species in singlet states are zero, whereas those for species in doublet states hover around 0.75, indicating insignificant influence of spin contamination on the estimation of activation barriers and the structures of all species.

Table 1. The spin contamination $<S^2>$ and the T1 diagnostics at the levels of B3LYP/6-311++G(3df,2p) and CCSD(T)/6-311++G(3df,2p), respectively.

Species	$<S^2>$	T1 diagnostics
allene (singlet)	0.0	0.011
propyne (singlet)	0.0	0.015
${}^{\bullet}OH$ (doublet)	0.75	0.023
TS1 (doublet)	0.76	0.027
TS2 (doublet)	0.76	0.025
${}^{\bullet}C_3H_3$ (doublet)	0.77	0.035
H_2O (singlet)	0.0	0.012

Thermochemical Properties. In order to check the accuracy of the calculations, the calculated thermodynamic property ($\Delta_f H_{298\ K}$) for all species involved in the reactions (1) and (2) was presented in Table 2 and compared to literature data. It can be seen from Table 2, the computed values agree well with the available literature data within their deviations, e.g., the difference between our values and the ATcT data does not exceed 1.0 kcal/mol. Such good agreements on the calculated thermodynamic parameter indicate that the methods used in this study are reasonable.

Table 2. Comparison of formation heats (in kcal/mol) of all species in this study with values derived from ATcT.

Species	$\Delta_f H_{298\ K}$ (this work)	$\Delta_f H_{298\ K}$ (ATcT)
Allene	46.02	45.43 ± 0.32
Propyne	44.91	44.38 ± 0.32
Propargyl	83.56	84.02 ± 0.39
H_2O	-57.35	-57.8 ± 0.026
${}^{\bullet}OH$	8.23	8.96 ± 0.026

Another point should be noted that the reactions of allene and propyne with the ${}^{\bullet}OH$ radicals occur not only via abstracting hydrogen atoms as discussed in this study, but also through addition of the ${}^{\bullet}OH$ radicals to different positions within the C_3H_4 structures. However, the OH-addition reactions have been thoroughly examined in the prior research of Zádor and Miller[15] and thus do not constitute the focus of this study. Also in their study, the H-abstraction paths are dominant in comparison with the OH-addition at high temperature regions.

4. KINETICS

Rate constants for the C_3H_4 + $^{\bullet}$OH reactions have been computed on the basis of the PES obtained at the CCSD(T)/aug-cc-pV(T+D)Z + ZPE level of theory. Because there are no intermediate states on the reacion channels (1) and (2), the rate constants for the initiation reaction have, therefore, been calculated by the TST using the CHEMRATE program based on the mechanisms shown in Figure 1. The predicted resutls are tabulated and plotted in Table 3 and in Figure 3, respectively.

Table 3. Rate coefficients (cm^3 $molecule^{-1}$ s^{-1}) of the reactions paths of allene and propyne with $^{\bullet}$OH radicals in the 300 – 2000 K range, where k_1 and k_2 are the values of (1) and (2).

T	k_1	k_2	T	k_1	k_2
300	5.40E-14	1.40.E-13	1200	8.24.E-12	7.96.E-12
400	1.64.E-13	3.08.E-13	1300	1.06.E-11	1.00.E-11
500	3.85.E-13	5.96.E-13	1400	1.35.E-11	1.24.E-11
600	7.58.E-13	1.03.E-12	1500	1.67.E-11	1.51.E-11
700	1.32.E-12	1.63.E-12	1600	2.03.E-11	1.81.E-11
800	2.11.E-12	2.42.E-12	1700	2.44.E-11	2.14.E-11
900	3.17.E-12	3.43.E-12	1800	2.90.E-11	2.50.E-11
1000	4.52.E-12	4.68.E-12	1900	3.41.E-11	2.90.E-11
1100	6.20.E-12	6.19.E-12	2000	3.96.E-11	3.34.E-11

It can be seen from Table 3 and Figure 3 that both the rate constants, k_1 and k_2 of the reactions (1) and (2), increase with rising temperatures. In addition, the k_1 value is smaller than the k_2 value over the temperature range from low to moderate (300 – 1000 K). However, at higher temperatures (≥ 1100 K), the value of k_2 gradually surpasses that of k_1. The observed difference amounts to approximately 19% at T = 2000 K. This is suitable because the energy barrier of the reaction (1) is higher than that of the reaction (2), 4 versus 2 kcal/mol. This calculated result further confirms that the reaction (2) proceeds more dominant than the reaction (1), consistent with the results shown in PES (see Figure 1).

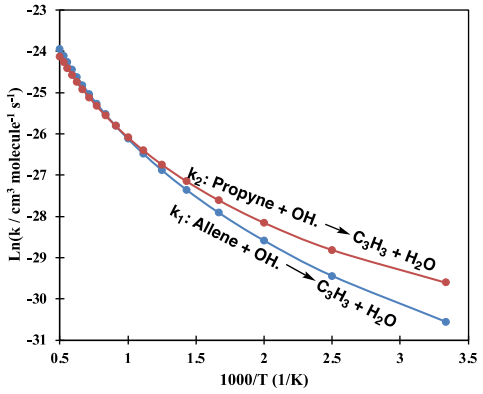

Figure 3. Rate constants of the reactions between allene and propyne and $^{\bullet}$OH radicals in the 300 – 2000 K interval.

5. CONCLUSION

In this work, the C_3H_4 + $^{\bullet}$OH reactions were optimized at the B3LYP/6-311++G(3df,2p) level. Energies for all the species have been refined at the CCSD(T)/aug-cc-pV(T+D)Z level. All the quantum calculations were performed by using the Gaussian 16. The pressure-independent rate constant has been calculated over the 300 - 2000 K range. At low and moderate temperature regions (T ≤ 1000 K), the rate of the propyne + $^{\bullet}$OH reaction is faster than that of the allene + $^{\bullet}$OH reaction. At higher temperatures, however, the latter is dominant.

6. REFERENCES

[1] Ollivier, J. L.; Dobrijévic, M.; Parisot, J. P. 2000. New photochemical model of Saturn's atmosphere. Planet. Space Sci. 48, 699-716.

[2] Moses, J. I.; Bézard, B.; Lellouch, E.; Gladstone, G. R.; Feuchtgruber, H.; Allen, M., 2000. Photochemistry of Saturn's Atmosphere. Icarus, 143, 244-298.

[3] Frenklach, M.; Taki, S.; Durgaprasad, M.B.; Matula, R. A. 1983. Soot formation in shock-tube pyrolysis of acetylene, allene, 1,3-butadiene. Combust. Flame, 54, 81.

[4] Fournet, R.; Bauge, J. C.; Battin-Leclerc, F. 1999. Experimental and modeling of oxidation of acetylene, propyne, allene and 1,3-butadiene. Int. J. Chem. Kinet., 31, 361-379.

[5] Hansen, N.; Miller, J. A.; Westmoreland, P. R.; Kasper, T.; Kohse-Höinghaus, K.; Wang, J.; Cool, T. A. 2009. Isomer-specific combustion chemistry in allene and propyne flames. Combust. Flame, 156, 2153-2164.

[6] Nguyen, T. N.; Trang, H. T. T.; Nguyen, N. T.; Pham, T. V. 2022. Computational study of the reaction of C_3H_3 with HNCO and the decomposition of C_4H_4NO radicals. Int. J. Chem. Kinet. 54, 447-460.

[7] Pham, T. V.; Trang, H. T. T. 2021. A theoretical study on mechanism and kinetics of the C_2H_3 + C_2H_3 recombination and the isomerization and dissociation of butadiene. Chem. Phys. 548, 111217.

[8] Pham, T. V.; Trang, H. T. 2023. Mechanistic and Kinetic Approach on the Propargyl Radical (C_3H_3) with the Criegee Intermediate (CH_2OO). Omega, 8, 16859-16868.

[9] Pham, T. V.; Trang, H. T.; Nguyen, H. M. T. 2022. Temperature and pressure-dependent rate constants for the reaction of the propargyl radical with molecular oxygen. ACS omega, 7, 33470-33481.

[10] Pham, T. V.; Trang, H. T. T. 2021. Theoretical investigation of the mechanisms and kinetics of the bimolecular and unimolecular reactions involving in the C_4H_6 species. J. Phys. Chem. A, 125, 585-596.

[11] Hidaka, Y.; Nakamura, T.; Miyauchi, A.; Shiraishi, T.; Kawano, H. 1989. Thermal decomposition of propyne and allene in shock waves. Int. J. Chem. Kinet. 21, 643.

[12] Wu, C.; Kern, R. 1987. Shock-tube study of allene pyrolysis. J. Phys. Chem. 91, 6291-6296. 436

[13] Davis, S.; Law, C.; Wang, H. 1998. In An experimental and kinetic modeling study of propyne oxidation, Symp. (Int.) Combust., Elsevier; 305-312.

[14] Giri, B. R.; Fernandes, R. X.; Bentz, T.; Hippler, H.; Olzmann, M. 2011. High-temperature kinetics of propyne and allene: Decomposition vs. isomerization. Proc. Combust.Inst 33, 267-272.

[15] Zádor, J.; Miller, J. A. 2015. Adventures on the C_3H_5O potential energy surface: OH + propyne, OH + allene and related reactions. Proc. Combust. Inst 35, 181-188.

[16] Bradley, J. N.; Hack, W.; Hoyermann, K.; Wagner, H. G. 1973. Kinetics of the reaction of hydroxyl radicals with ethylene and with C_3 hydrocarbons. J. Chem. Soc., Faraday Trans. 69, 1889-1898.

[17] Atkinson, R.; Perry, R.; Pitts Jr, J. 1977. Absolute rate constants for the reaction of OH radicals with allene, 1, 3-butadiene, and 3-methyl-1-butene over the temperature range 299–424° K. J. Chem. Phys. 67, 3170-3174

[18] Taylor, S. E.; Goddard, A.; Blitz, M. A.; Cleary, P. A.; Heard, D. E. 2008. Pulsed Laval nozzle study of t1977, he kinetics of OH with unsaturated hydrocarbons at very low temperatures. Phys. Chem. Chem. Phys. 10, 422.